An improved mathematical modeling to simulate metallization screen pattern trend for silicon solar cell

Lin Jiang, Weiming Zhang, Tracy Guo, David Kapp, Li Yan, Larry Wang

Heraeus Precious Metals North America Conshohocken, LLC, Photovoltaic Business Unit

24 Union Hill Road, W. Conshohocken, PA 19428, USA

***Abstract* — the series resistance calculation based on H-type model has been widely used to understand power loss mechanism in semiconductor solar cell, and one of its popular applications is to predict optimal metallization screen printing pattern. The disadvantage of this model is that it is not accurate to estimate the relationship of screen pattern trend vs. cell efficiency, since it is based on an ideal rectangular finger shape, which does not exist in present regular screen printing process. In this work, a revised model is proposed to simulate the contact resistant power loss in multi-crystalline silicon solar cell. Improved accuracy of the new model is found by comparing the simulation results to the I-V testing data of multi-crystalline silicon solar cell printed with Heraeus 96XX front Ag paste.**

***Index Terms* — silicon, solar cell, series resistance, metallization**

I. INTRODUCTION

As the dominate solar-cell metallization technique in present silicon solar cell manufacturing, screen printing has superior cost saving over other technologies. In the past decade, paste suppliers have been responsible for steady improvements in cell performance and reduction in dollar-per-watt costs, and nowadays are facing more challenges to further cost reduction and to improve cell efficiency. Therefore, a more accurate understanding of optimal grid pattern trend vs. cell efficiency is needed.

The popular H-type grid pattern (Fig.1) for series resistance simulation is based on the assumptions [1]: (i) the cell is uniformly illuminated; (ii) the photo current flows uniformly into the surface sheet and spreads laterally to the gridline and then collected by bus bar; (iii) grid line fingers and bus bar cross section area are rectangular; (iv) fingers are uniform; (v) finger width is wider than transfer lifetime L_T by 1.5 times.

However, in practice screen printed fingers seldom hold ideal rectangular shape, and are usually not uniform. In addition, the finger width in present cell manufacture processes are significantly reduced, from 100~200 μm three years ago, to no longer wider than 1.5 times of L_T today. These differences will cause discrepancies between I-V tested series resistance values and calculated values, hence, lead to inaccurate cell performance estimates. In this work, a revised model is proposed to simulate the series resistant power loss in multi-crystalline silicon solar cell, greatly reduced the difference between the calculation and tested results.

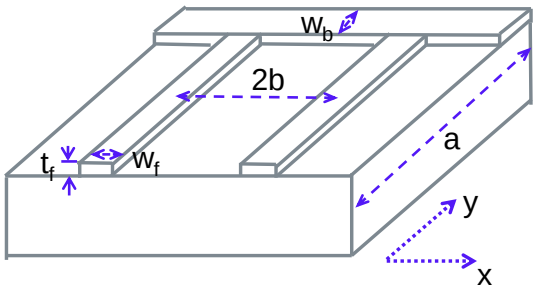

Fig.1 H-type grid pattern for rectangular solar cell

II. REVISED MODEL DESCRIBTION

In the revised model, we begin at the unit cell with *a* units long and *2nb* units wide, with *n* the number of grid fingers, and *2b* the distance between the centers of neighboring grid fingers. The entire rectangular solar cell is then composed of repeated unit cells. The power loss due to series resistance is associated with current travelling through the emitter, the contact resistance, gridline fingers, bus bars, and through the base of cells. For diffused emitter layer and base, D. Meier gave the expressions as below [1],

$$P_{sheet} = \frac{2}{3} J_L^2 \, nab^3 R_{sheet} \qquad (1)$$

$$P_{base} = 2 J_L^2 \, nabl \rho_{base} \qquad (2)$$

Where J_L is the light-generated current density, R_{sheet} is the emitter sheet resistance, l is the base region thickness, and ρ_{base} is the semiconductor base resistivity.

Since the screen printed grid finger shape are not ideally rectangular, we revise grid finger cross section area by a trapezoid shape or Gaussian shape to simulate the practical screen printing finger shape, as shown in Fig.2-(a)&(b).

The element resistance *dR* of the grid finger is given by,

$$dR = (\rho_f / A)\, dy \qquad (3)$$

Where A is the cross-sectional area of the grid finger, and ρ_f is the gridline resistivity.

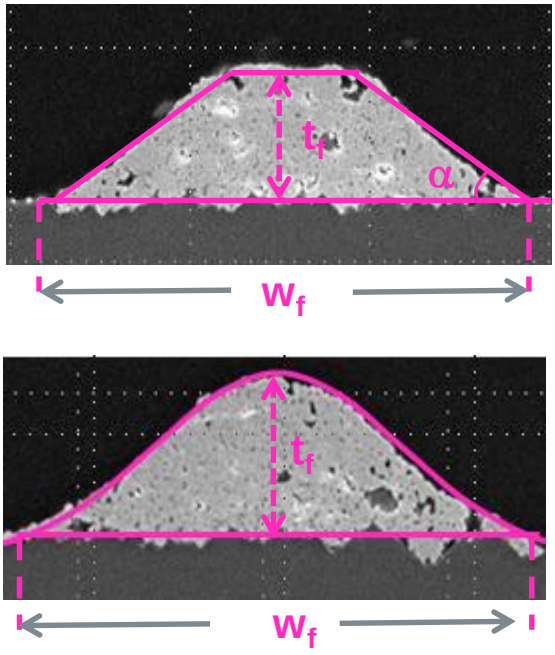

Fig.2 Screen printing grid finger cross-section area:
(a) Trapezoid shape, (b) Gaussian shape

For a trapezoid grid finger as shown in Fig.2-(a), cross-section area is,

$$A_1 = (W_f - \frac{t_f}{tg\alpha})t_f \qquad (4)$$

Where W_f is the finger width, t_f is the finger height, and tgα is the slope of finger side-wall. For a given tgα and W_f, the finger height range is $0 < t_f < 0.5 W_f\, tg\alpha$.

For a Gaussian shape grid finger like Fig.2-(b), the profile of finger can be described as equation (5), with the peak of t_f and the standard deviation of σ,

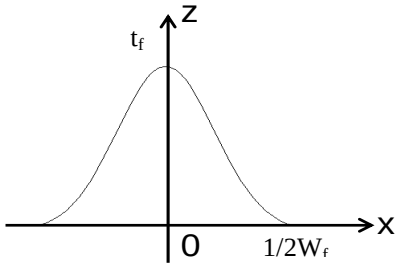

Fig.3 Gaussian profile of grid finger

$$\varphi(x) = t_f e^{-\frac{x^2}{2\sigma^2}} \qquad (5)$$

The area within Gaussian profile can be obtained in equation (6), and the full width at half maximum (FWHM) is related to the standard deviation σ according to equation (7),

$$A_2 = \int_{-\infty}^{+\infty} \varphi(x)dx = t_f \sigma \sqrt{2\pi} \qquad (6)$$

$$FWHM = 2\sqrt{2ln2}\,\sigma \qquad (7)$$

If we define s = FWHM/W_f, the cross-section area yields,

$$A_2 = \frac{s w_f t_f \sqrt{\pi}}{2\sqrt{ln2}} \qquad (8)$$

Substitute equation (4) and (8) into equation (3), the element resistance of trapezoid and Gaussian shape grid fingers are given in equation (9) and (10), respectively,

$$dR1 = \frac{\rho_f}{(W_f - \frac{t_f}{tg\alpha})t_f}\, dy \qquad (9)$$

$$dR2 = (\frac{2\rho_f \sqrt{ln2}}{s w_f\, t_f \sqrt{\pi}})\, dy \qquad (10)$$

Since the power loss associated with current flow along the grid finger is (11),

$$P_{finger} = n \int_0^a I^2(y) dR \qquad (11)$$

$$I(y) = 2b(a - y)J_L \qquad (12)$$

The power loss of grid fingers with trapezoid or Gaussian shape cross-section areas can be written as (13) and (14), respectively,

$$P_{finger1} = \frac{4}{3} J_L^2 n a^3 b^2 \rho_f \frac{1}{(w_f - \frac{t_f}{tg\alpha})t_f} \qquad (13)$$

$$P_{finger2} = \frac{8}{3} J_L^2 n a^3 b^2 \rho_f \frac{\sqrt{ln2}}{s\, w_f\, t\, \sqrt{\pi}} \qquad (14)$$

Now we consider another difference between practical grid fingers to the ideal ones, uniformity. As shown in Fig. 4, the roughness of the real gridline fingers can cause a disagreement in line resistance to the ideal smooth case. Since the rough surface is mainly formed by the wire mesh of the screen, the peaks and valleys are relatively regular. If the valley area is represented by a resistance R_1, and the peak area resistance by R_2, as shown in Fig.4 (b), the resistances of a uniform and non-uniform finger can be described by (16) and (17), respectively.

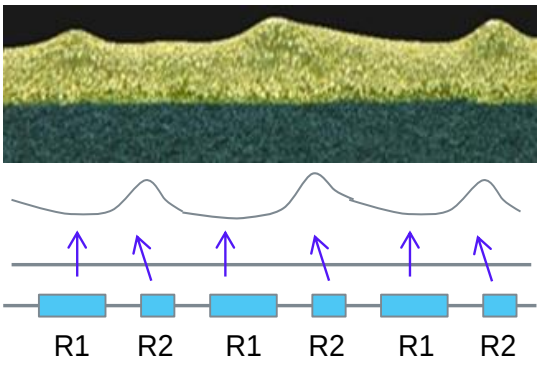

Fig.4 Resistance model for finger roughness

$$f = \frac{R2}{R1} \tag{15}$$

$$R_{uniform} = R1 + R1 + \cdots = 2MR1 \tag{16}$$

$$R_{non-uniform} = R1 + R2 + R1 + R2 + \cdots = M(1+f)R1 \tag{17}$$

$$R_{non-uniform} = \frac{1+f}{2} R_{uniform} \tag{18}$$

If the ratio of peak and valley resistance is defined by roughness coefficient $f=R_2/R_1$, then the finger power loss expression (13) and (14) can be modified as (19) and (20), respectively.

$$P_{finger1} = \frac{4}{3} J_L^2 n a^3 b^2 \rho_f \frac{1+f}{(w-\frac{t_f}{tg\alpha})t_f} \tag{19}$$

$$P_{finger2} = \frac{8}{3} J_L^2 n a^3 b^2 \rho_f \frac{\sqrt{ln2}\,(1+f)}{s\,w\,t\sqrt{\pi}} \tag{20}$$

In addition to emitter, base, fingers, the fourth contribution to power loss is the contact resistance. Considering the transfer length concept, the contact resistance [2] is given by,

$$R_c = \frac{L_T R_{sheet}}{a} \coth(\frac{W_f}{2L_T}) \tag{21}$$

Where L_T is the transfer length [3],

$$L_T = (\rho_c / R_{sheet})^{1/2} \tag{22}$$

In the case that $W_f/2 > 1.5L_T$, $coth(W_f/(2L_T)) \cong 1$, and $R_c = \rho_c/(L_T a)$; so contact resistance is independent of grid width W_f. However, with the present trend to reduce finger width for multi-crystalline and mono-crystalline silicon solar cell , typically around 40~90 μm, this limit is not valid. In hence, the finger with will influence the contact resistance value, as shown in equation (21).

Since the power loss associated with front contact resistance is $2nI^2R_c$, and $I=J_Lab$, so the expression of contact resistance dissipated power yields,

$$P_{contact} = 2J_L^2 nab^2 (\rho_c R_{sheet})^{1/2} \coth(\frac{w_f}{2}\sqrt{\frac{R_{sheet}}{\rho_c}}) \tag{22}$$

The back contact is covered by large area of metal (Al) and can be ignored [1] compared to other series segment.

For bus-bar, we can also use a trapezoid shape to describe the cross-section area. In the unit cell, W_b is half of bus-bar width (Fig. 5), so the bus-bar power loss is described as (23),

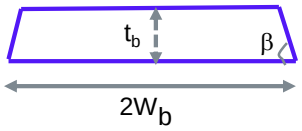

Fig. 5 Cross section area of bus-bar

$$P_{bus} = \frac{4}{3} J_L^2 n^3 a^2 b^3 \frac{\rho_f\, tg\beta}{(2tg\beta W_b - t_b)t_b} \tag{23}$$

Since the bus-bar width is much wider than that of finger, it is easier to print the bus-bar with a rectangular cross-sectional area, and the expression can be deduced to (24),

$$P_{bus} = \frac{2}{3} J_L^2 n^3 a^2 b^3 \frac{\rho_f}{W_b t_b} \tag{24}$$

If the energy conversion efficiency of solar cell is η, and the power density is P_L, the front metal shadowing caused power loss is

$$P_{shadow} = P_L \eta\, n\, [(a - w_b)w_f + 2bw_b] \tag{25}$$

The overall power loss is the sum of power loss from the emitter, contact, grid fingers, bus-bar, base, plus the shadowing loss,

$$P_{Rs} = P_{sheet} + P_{contact} + P_{finger} + P_{bus} + P_{base} \tag{26}$$

$$P_{all} = P_{Rs} + P_{shadow} \tag{27}$$

Equations (1), (2), (19), (20), (22), (23), and (25) are then normalized to unit cell area $2nab$, and the summary of expressions are listed in TABLE-I.

TABLE I
SUMMARY OF POWER LOSS EXPRESSION

Power Loss Factors	Normalized expression
Emitter	$P_{sheet} = \frac{1}{3} J_L^2 \, b^2 R_{sheet}$
Front Contact	$P_{contact} = J_L^2 b (\rho_c R_{sheet})^{1/2} \coth(\frac{w_f}{2}\sqrt{\frac{R_{sheet}}{\rho_c}})$
Grid finger	$P_{finger1} = \frac{2}{3} J_L^2 a^2 b \rho_f \frac{1+f}{(w - \frac{t_f}{tg\alpha}) t_f}$
Grid finger	$P_{finger2} = \frac{4}{3} J_L^2 a^2 b \rho_f \frac{\sqrt{ln2(1+f)}}{s w_f t_f \sqrt{\pi}}$, $s = \frac{FWHM}{w_f}$
Bus-bar	$P_{bus} = \frac{2}{3} J_L^2 n^2 b^2 a \frac{\rho_f \, tg}{(2tg\beta \, W_b - t_b) t_b}$
Base	$P_{base} = J_L^2 \, l \rho_{base}$
Shadowing	$P_L \eta \, [\frac{(a - w_b) w_f}{2ab} + \frac{w_b}{a}]$

The cell series resistance, normalized to unit area is,

$$r_s = {P_{Rs}}/{J_L^2} \qquad (28)$$

The segment of each cell series resistance, normalized to unit area, can be achieved by substituting P_{Rs} with the corresponding power loss factor from TABLE I.

III. RESULTS AND DISCUSSIONS

Two standard multi-crystalline silicon solar cells were printed using Heraeus 96XX front Ag paste with a 3 bus-bar 85-finger line screen, and the back metallization was formed by a commercial Al paste.

The related device and material parameters are listed in TABLE-II. Using these parameters, we can estimate the normalized power loss factors in TABLE-I and the corresponding cell series resistance.

TABLE-III shows the comparison of estimated series resistance values to the I-V tested values. When finger roughness coefficient f =1, i.e. grid fingers are uniform; the estimated series resistance using rectangular, trapezoid , and Gaussian cross-section area finger modes for cell-1 are 0.41, 0.44, and 0.48 Ω-cm^2, values much smaller than the tested value 0.66 Ω-cm^2. When the roughness effect is taken into consideration (f=3.25), the calculated values increased to 0.50 , 0.56, and 0.66 Ω-cm^2, correspondingly, and are much more closer to the tested value.

TABLE II
CELL 1&2 DEVICE AND MATERIAL PARAMTERS

Parameters	Cell-1	Cell-2
R_{sheet} (Ω/□)	81.9	80.6
t_f (μm)	17.2	17.4
w_f (μm)	78.3	84.2
t_b (μm)	15.5	15.7
W_b (mm)	0.75	0.75
η	17.6	17.4
a (cm)	2.55	
b (cm)	0.091	
ρ_c (Ω-cm^2)	2.3×10^{-3}	
ρ_f (Ω-cm)	2.7×10^{-6}	
l (μm)	170	
$S=FWHM/w_f$	0.49	
α	40 °	
J_L (mA/cm^2)	38.2	

TABLE III
CALCULATED &TESTED SERIES RESISTANCE

Items	Cell-1		Cell-2	
	1	3.25	1	3.25
Rs-Rectangular (Ω-cm^2)	0.41	0.50	0.40	0.48
Rs-Trapezoid (Ω-cm^2)	0.44	0.56	0.42	0.53
Rs-Gaussian (Ω-cm^2)	0.48	0.66	0.47	0.63
Rs- Tested (Ω-cm^2)	0.66		0.58	

The relationship of series resistance and roughness coefficient f for three types of finger models are shown in Fig.6. The results suggest that finger uniformity is very important, because the series resistance value is sensitive to finger roughness, hence cell performance will be affected.

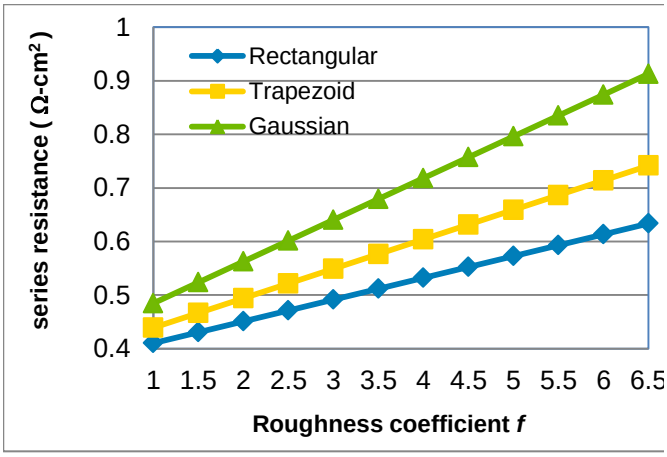

Fig.6 series resistance vs. roughness coefficient

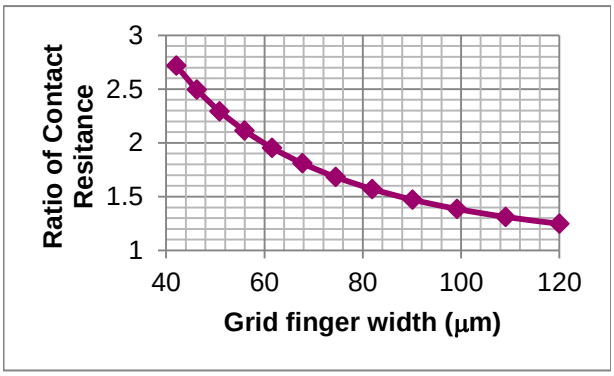

Fig. 7 Finger width influence on contact resistance

Fig. 7 presents the influence of grid finger width on contact resistance. The vertical axis is the ratio of contact resistance estimated using the revised contact model in TABLE-I and contact resistance without finger width influence, i.e.$coth(W_f/(2L_T))\cong 1$. The results show that when finger width is reduced, the contact resistance becomes larger. Therefore, its influence on cell performance will be more sensitive than wider fingers.

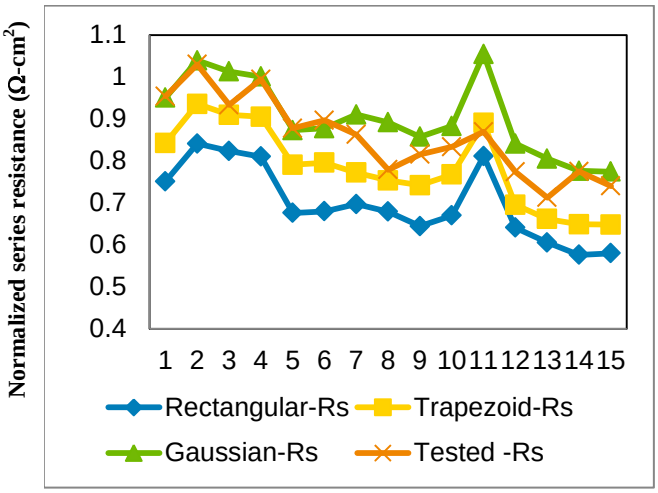

Fig. 8 Estimated and tested series resistance values of 15 samples

Finally, more samples (15 cells) were printed with various experimental pastes, and series resistance values are compared to the estimated ones. Fig.8 shows normalized cell series resistance value r_s of three finger type models and the I-V test results. From the chart, it is found that 8 samples showed best match using Gaussian finger model, 3 samples showed best match using Trapezoid finger model, and 5 samples are between Gaussian and Trapezoid finger shape.

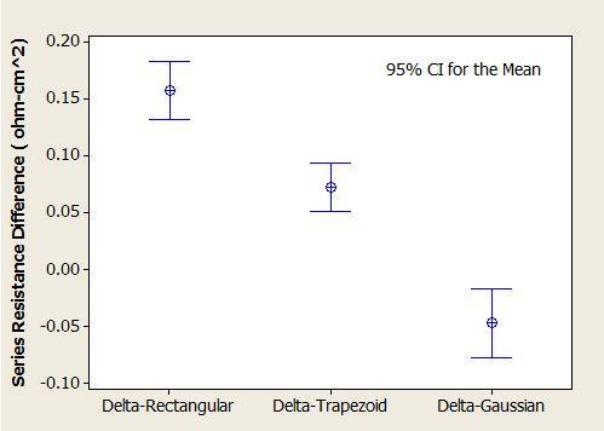

Fig. 9 Interval plot of series resistance difference between tested value and estimated value

The difference between the estimated results and the tested value is summarized in Fig. 9, where Delta-Rectangular, Delta-Trapezoid, and Delta Gaussian represents the difference of corresponding values to tested values. The accuracy, i.e. estimated value divided by tested value, was improved by 10%~20%.

IV SUMMARY

Three modifications are applied on conventional H-type grid pattern power loss model: 1) Gaussian or trapezoid cross-section area is used according to the practical screen printing finger shapes; 2) Non-uniformity effects are taken into consideration in the model; 3) The influence of finger width on contact resistivity was included. Real I-V test data is used to verify the estimated data, and the accuracy of the model is found to be improved.

REFERENCES

[1] Daniel L. Meier, Dieter K. Schroder, "Contact Resistance: Its measurement and Relative Importance to Power Loss in a Solar Cell", IEEE Trans. Electron Devices, vol. 31, no.5.pp. 647-653, 1984

[2] G.K.Reeves and H. B. Harrison, "Obtaining the specific contact resistance from transmission line model measurements", IEEE Electron Device Lett., vol. EDL-3, pp. 111-113, 1982

[3] D.Schroder and D. Meier, "Solar Cell Contact Resistance – A Review", IEEE Trans. Electron Devices, vol. 31, no.5.pp. 637-647, 1984